Synthesis

All reagents and solvents were obtained from commercial sources and used without further treatment. Hsal (122 mg, 1.0 mmol) and NEt_3 (0.2 ml, 1.0 mmol) were added to MeCN (20 ml) and the solution kept under stirring for 10 minutes, followed by addition of $Co(OAc)_2{\cdot}4H_2O$ (249 mg, 1.0 mmol). The resultant pink solution was left under stirring for 30 minutes during which time no colour change was observed. The solution was then filtered and layered with Et_2O (40 ml). Pink crystals of **1**·16MeCN formed over 3 days in ~30% yield. Anal. Calcd (found) for **1**: C, 45.21; H, 3.37. Found: C, 44.93, H, 3.23.

Physical Measurements

Elemental analyses (C, H, N) were performed by the University of Ioannina microanalysis service.

X-ray diffraction

Single crystal X-ray diffraction data were collected on a Bruker D8 VENTURE diffractometer (University of Crete), equipped with a PHOTION II CPAD detector. Crystal data for **1** (CCDC 2178060): $C_{176}Co_{16}H_{208}O_{72}$, M = 4418.29 g/mol, tetragonal, space group $P4/n$ (no. 85), a = 29.9250(6) Å, c = 11.2727(3) Å, V = 10094.8(5) Å^3, Z = 2, T = 200(2) K, μ(CuKα) = 10.704 mm^{-1}, *Dcalc* = 1.454 g/cm^3, 28843 reflections measured (4.176° ≤ 2Θ ≤ 136.522°), 9197 unique (R_{int} = 0.0378, R_{sigma} = 0.0405) which were used in all calculations. The final R_1 was 0.0435 (I > 2σ(I)) and wR_2 was 0.1257 (all data).

Powder X-ray diffraction data for **1** were collected using a Bruker D8 ADVANCE with copper radiation at 40 kV, 40 mA and a Johansson monochromator, 2 mm divergence slit and 2.5 degree Soller slits on the incident beam side. LynxEye detector and Bruker DIFFRAC software. Diffraction measured from 2θ = 3° - 30°; step size, 0.0101°. Samples were loaded into quartz capillaries with a 1 mm inside diameter and measured while spinning.

Magnetic Measurements

Magnetic susceptibility data were collected on a polycrystalline sample of **1** on a Quantum Design Dynacool PPMS equipped with a 9 T magnet in the temperature range 300 - 2.00 K. Diamagnetic corrections were applied to the observed paramagnetic susceptibilities using Pascal's constants.

Computational Details

To estimate the intramolecular magnetic exchange interactions in **1** we have employed Density Functional Theory (DFT) in Gaussian 09 on a model complex (**Model 1**) created from the ASU of **1**.[1] We have performed pairwise exchange interaction calculations by keeping only the two paramagnetic centres of interest in **Model 1**, replacing the remaining Co^{II} ions with diamagnetic Zn^{II} ions. This method is known to reproduce experimental magnetic exchange values for systems with weak intramolecular magnetic exchange interactions ($J \leq 10$ cm^{-1}).[2] The hybrid B3LYP functional[3] has been used together with the TZV basis set for Co, SVP basis set for Zn, O and SV basis set for C and H atoms.[4] We have employed Noodleman's broken symmetry methodology.[5]

To calculate the zero field splitting (zfs) parameters for each Co^{II} centre in the ASU we have used the ORCA software suite (version ORCA 4.0).[6] The zeroth-order regular approximation (ZORA) method in combination with the ZORA contracted version of basis set (ZORA-def2-TZVP for Co and ZORA-def-SVP for rest of the elements)[7] is known to be a reliable methodology to estimate zfs parameters. We have used the resolution of identity (RI) approximation. During state-average complete active space self-consistent field (SA-CASSCF) calculations we have considered seven electrons in five d-orbitals (CAS (7 electrons / 5 3d-orbitals)) in the active space with ten triplet and fifteen singlet roots. We have used 2^{nd} order N-electron valence perturbation theory to estimate the zero-field splitting parameter as well as to consider the dynamic correlation.[8] We have used integration Grid 6 for Co, Grid 5 for O and Zn, and Grid 4 for the remaining elements.

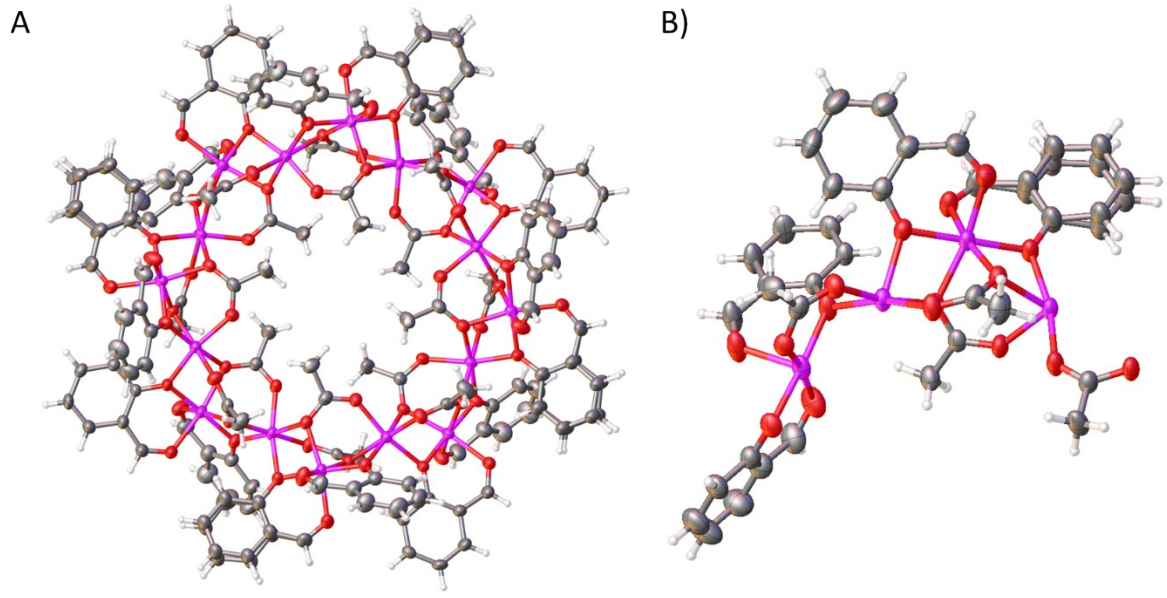

Fig. S1. (A) Molecular structure of **1** viewed perpendicular to the [Co_{16}] plane. (B) Asymmetric unit of **1**. Both figures presented with atomic displacement parameters. Colour code: Co = pink, O = red, C = black, H = white.

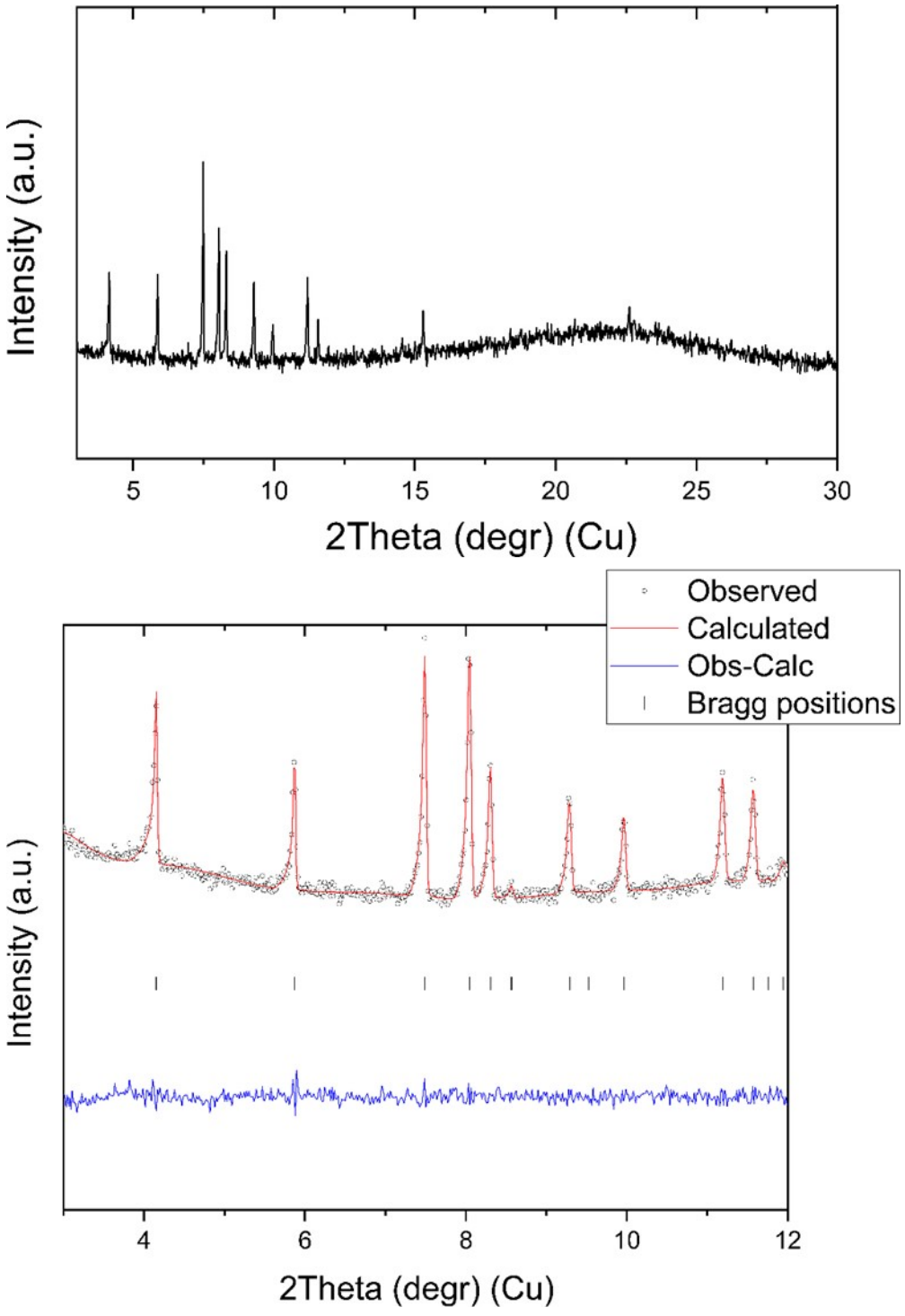

Fig. S2. Powder diffraction data for compound **1** (top). Refinement of the experimental diffraction data of **1** collected at room temperature by using the Pawley method and the single-crystal structural model as starting parameters (bottom). Experimental (black circles), calculated (red line), difference plot [(Iobs−Icalc)] (blue line) and Bragg positions (black ticks). Tetragonal, P_4/n; a = 30.0816 Å; c = 11.7914 Å; $\alpha = \beta = \gamma = 90°$; R_{exp} = 0.85 %, R_{wp} = 1.06 %, GoF = 1.25.

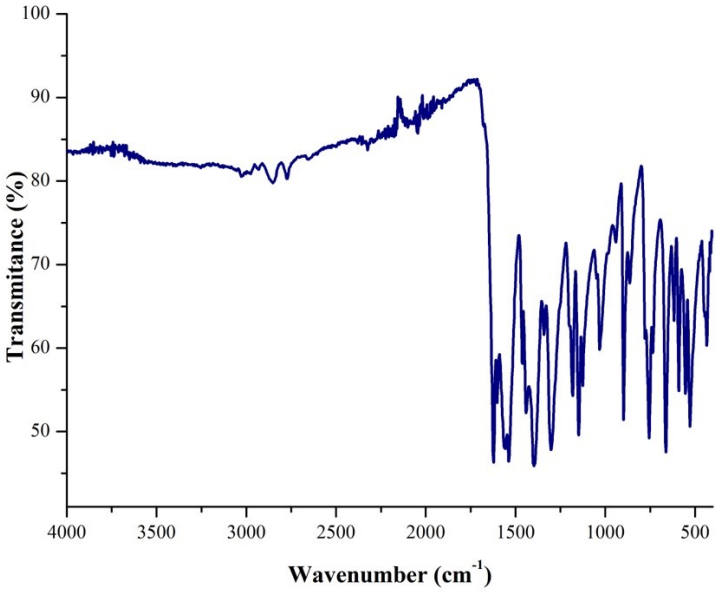

Fig. S3. FT-ATIR spectrum of **1**

Table S1. Bond Valence Sum (BVS) calculations for the metal ions in **1**.

	Co(II)	**Co(III)**
Co1	2.16	2.20
Co2	1.94	1.97
Co3	2.12	2.16
Co4	1.96	2.00

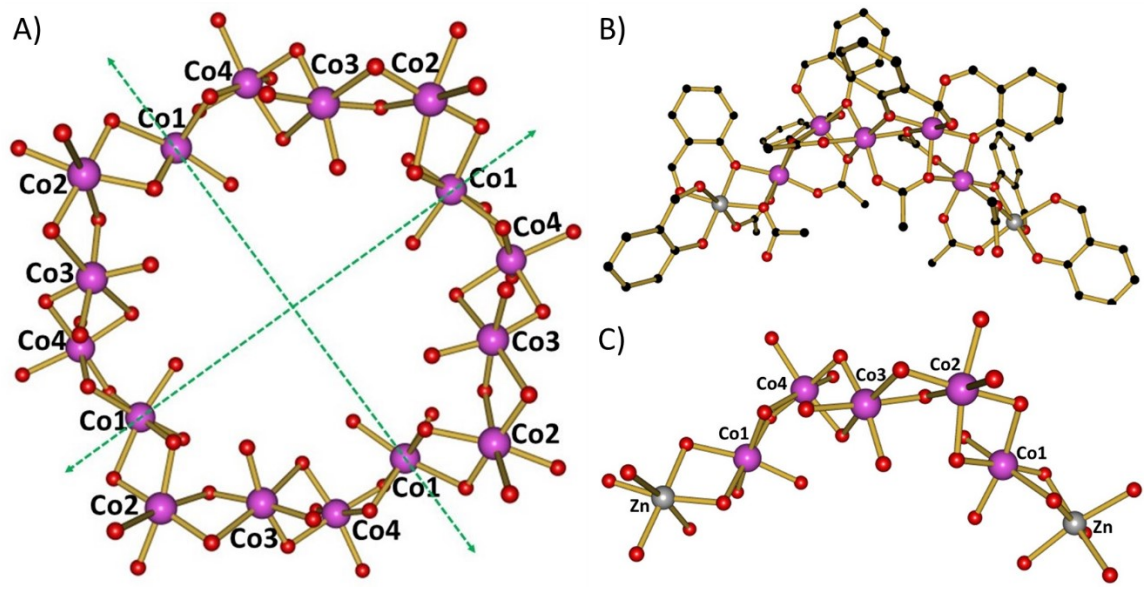

Fig. S4. (A) metal-oxygen core of complex **1**, highlighting the ASU. The full structure (B) and metal-oxygen core (C) of **Model 1**. The latter is the ASU of complex **1**. Colour code: Co = pink, O = red, Zn = silver and C = black. H atoms are removed for clarity.

Table S2. Pertinent structural parameters for **1** alongside the DFT computed magnetic exchange interactions.

	Average Co-O-Co angle (°)	Average Co-O distance (Å)	Average Co-O-Co-O angle (°)	Average Co···Co distance (Å)	J (cm^{-1}) nearest neighbour
Co1-Co2	95.2	2.100	21.1	3.100	+3.2
Co2-Co3	96.4	2.089	22.1	3.113	+1.7
Co3-Co4	95.7	2.096	22.2	3.104	+2.5
Co4-Co1	96.8	2.084	22.4	3.114	+3.8

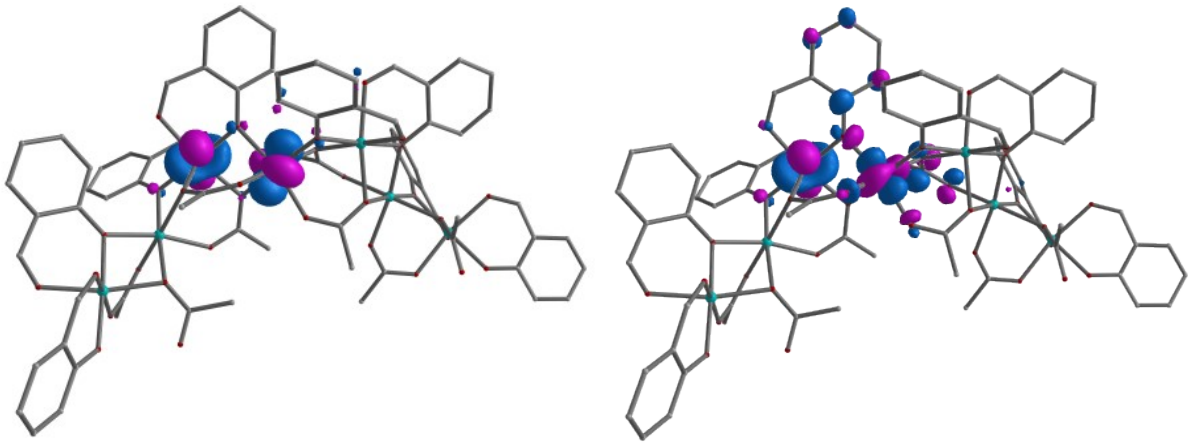

$\langle Co(\alpha)d_{yz}||Co(\beta)d_{yz}\rangle = 0.012$

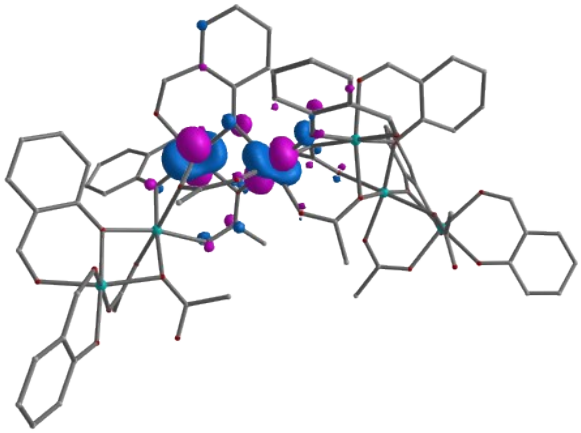

$\langle Co(\alpha)d_{yz}||Co(\beta)d_{x^2-y^2}\rangle = 0.020$

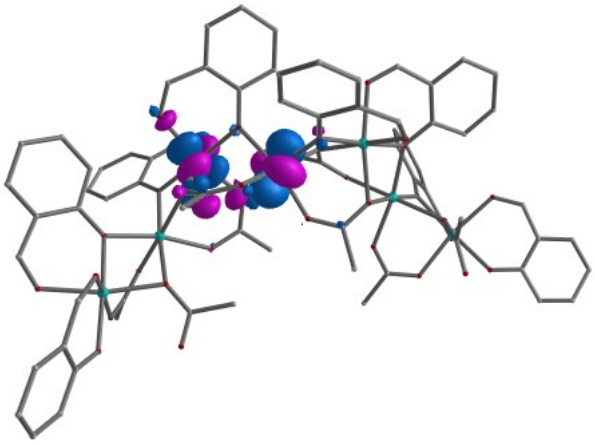

$\langle Co(\alpha)d_{yz}||Co(\beta)d_{z^2}\rangle = 0.068$

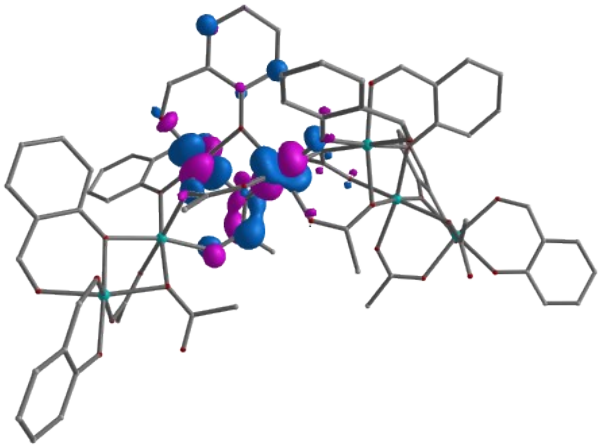

$\langle Co(\alpha)d_{x^2-y^2}||Co(\beta)d_{yz}\rangle = 0.000$

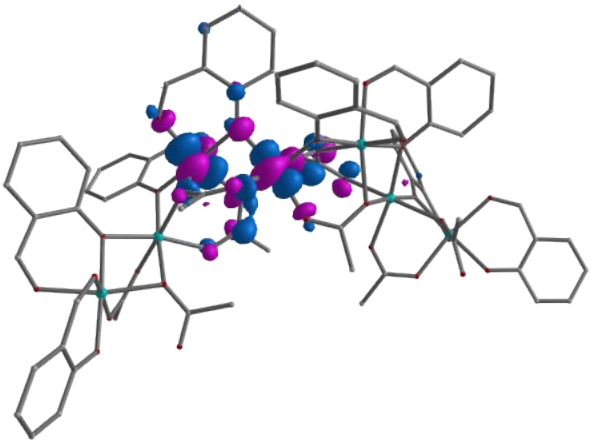

$\langle Co(\alpha)d_{x^2-y^2}||Co(\beta)d_{z^2}\rangle = 0.017$

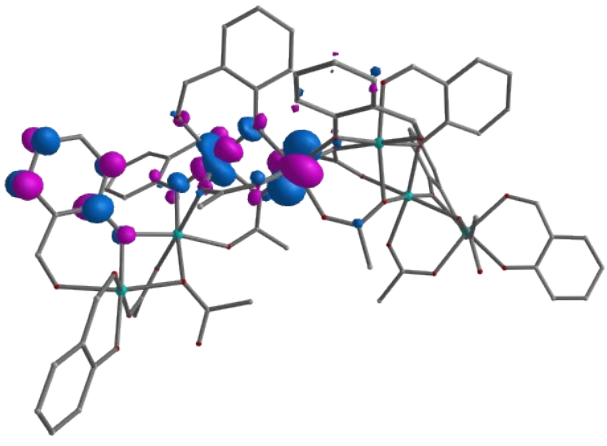

$\langle Co(\alpha)d_{x^2-y^2}||Co(\beta)d_{x^2-y^2}\rangle = 0.044$

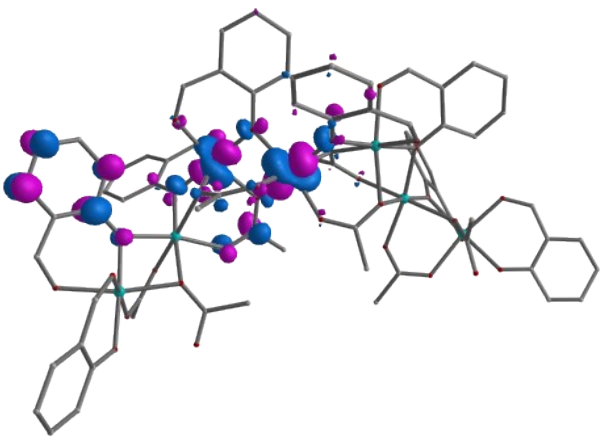

<Co(α)d_{z^2}||Co(β)d_{yz}> = 0.003

<Co(α)$d_{x^2-y^2}$||Co(β)d_{z^2}> = 0.053

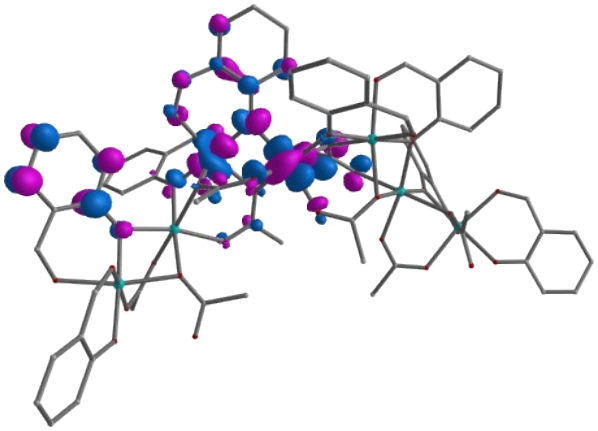

<Co(α)d_{z^2}||Co(β)$d_{x^2-y^2}$> = 0.075

Fig. S5. DFT computed overlap integral values together with the representative MO diagram. Three intermediate (green text) and six small (black text) overlap interactions are computed.

Table S3. SHAPE analysis[9] performed on each Co^{II} ion in the ASU of **1**.

```
HP-6            1 D6h   Hexagon
PPY-6           2 C5v   Pentagonal pyramid
OC-6            3 Oh    Octahedron
TPR-6           4 D3h   Trigonal prism
JPPY-6          5 C5v   Johnson pentagonal pyramid J2

Structure [ML6 ]          HP-6        PPY-6        OC-6        TPR-6       JPPY-6
 Co1-Co16         ,      30.213,      24.540,      1.059,      13.315,      27.817
 Co2-Co16         ,      29.535,      23.730,      0.969,      12.691,      27.326
 Co3-Co16         ,      29.945,      24.306,      1.095,      13.051,      27.604
 Co4-Co16         ,      29.275,      24.250,      0.878,      13.275,      27.920
```

Table S4. *Ab initio* NEVPT2 estimated anisotropy parameters (*g*, *D* and *E*/*D*) for each Co^{II} ion in the ASU of **1**. We include the d orbital energies, d_{yz} = grey, d_{xz} = pink, d_{xy} = blue, d_{z^2} = red and $d_{x^2-y^2}$ = black.

	g_{xx}, g_{yy}, g_{zz} (g_{iso})	D (cm^{-1})	E / D	NEVPT2 computed d orbital energies (cm^{-1})
Co1	1.902, 2.439, 2.930 (2.424)	87.1	0.24	**0.0**, **294.3**, **842.8**, **6467.4**, **8226.7**
Co2	2.057, 2.408, 2.562 (2.342)	41.2	0.23	**0.0**, **75.1**, **1135.2**, **7159.2**, **9955.8**
Co3	1.880, 2.471, 2.928 (2.426)	88.5	0.22	**0.0**, **287.4**, **892.4**, **6356.9**, **8275.0**
Co4	2.050, 2.437, 2.576 (2.354)	44.6	0.20	**0.0**, **105.5**, **1001.4**, **7256.7**, **10037.3**

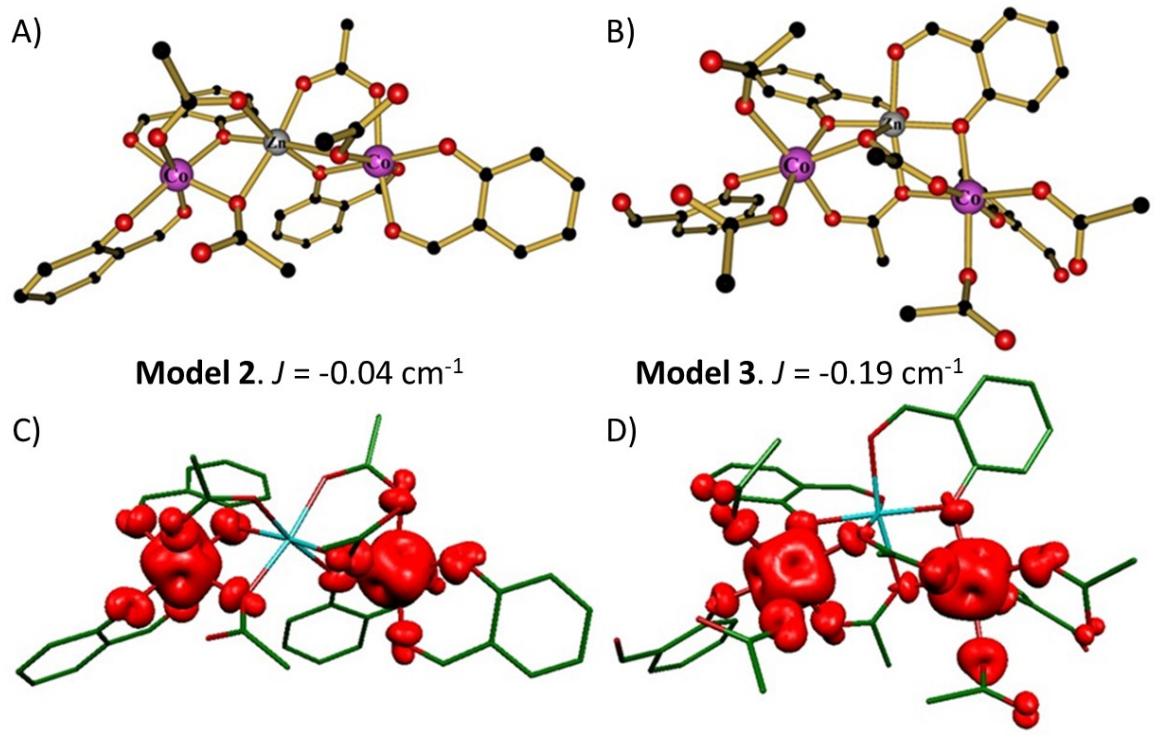

Fig. S6. The trimetallic Co-Zn-Co models employed to estimate the two unique next-nearest neighbour magnetic interactions present in **1**. a) **Model 2** where both next-nearest neighbour magnetic centres are not directly bridged by any functional group, and (b) **Model 3** where both centres are bridged via two syn-anti-O-C-O(carboxylate) groups. (c-d) Spin density plots for models **Model 2** and **Model 3**, respectively. Analysis further supports the presence of little/no magnetic interaction for the former and a very small interaction through the syn-anti-O-C-O(carboxylate) pathway for the latter.

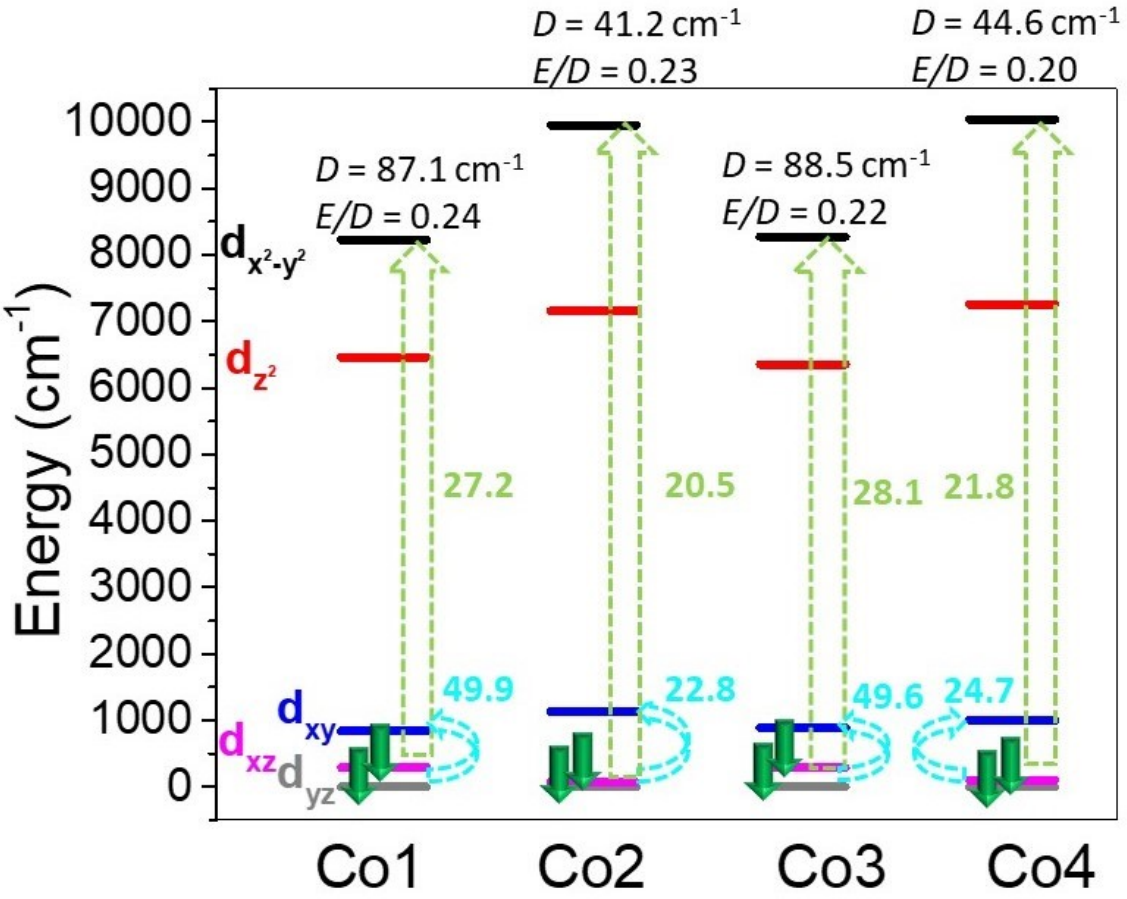

Fig. S7. *Ab initio* NEVPT2 computed d-orbital splitting for each Co^{II} ion in the ASU of **1**. Easy-plane anisotropy (+*D*) can be attributed to the electronic transitions between orbitals with different m_L levels ($d_{xz/yz} \rightarrow d_{xy/x^2-y^2}$). Note that two electronic transitions $d_{xz/yz} \rightarrow d_{xy}$ (cyan curly arrow) and $d_{xz/yz} \rightarrow d_{x^2-y^2}$ (light green straight arrow) give positive *D* values with the dominant contribution arising from the $d_{xz/yz} \rightarrow d_{xy}$ electronic transition. The magnitude of *D* is correlated to the energy separation between the orbitals involved in the electronic transition (i.e. between $d_{yz/xz}$ and d_{xy/x^2-y^2}).

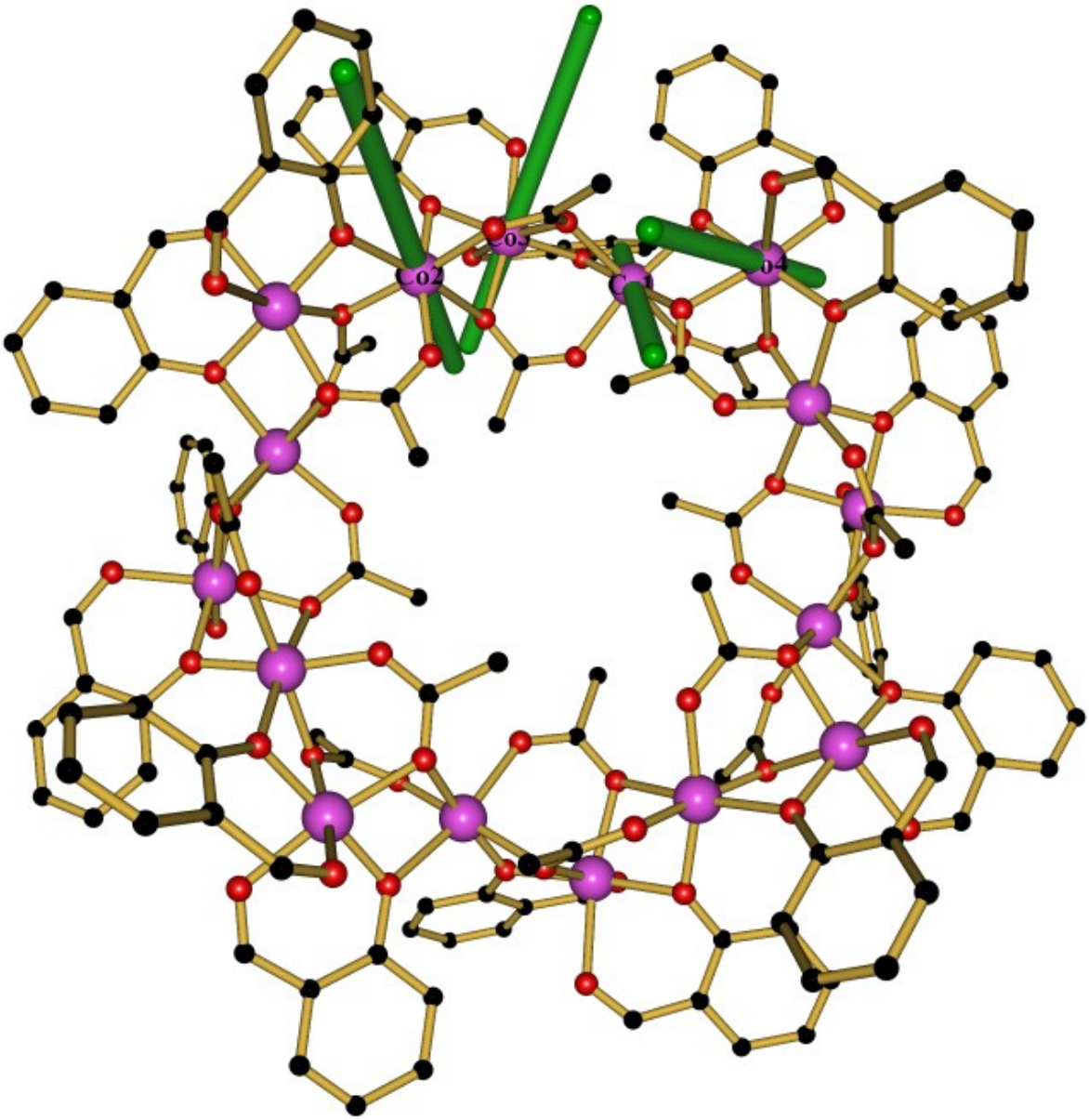

Fig. S8. The NEVPT2 computed D_{zz} axis (green bars) for Co1-Co4 centres in **1**. The non-collinearity of the D_{zz} axis of the Co^{II} centres can be attributed to the non-planar sinusoidal arrangement of metal centres.

References:

1. M. J. Frisch, G. W. Trucks, H. B. Schlegel, G. E. Scuseria, M. A. Robb, J. R. Cheeseman, G. Scalmani, V. Barone, B. Mennucci, G. A. Petersson, H. Nakatsuji, M. Caricato, X. Li, H. P. Hratchian, A. F. Izmaylov, J. Bloino, G. Zheng, J. L. Sonnenberg, M. Hada, M. Ehara, K. Toyota, R. Fukuda, J. Hasegawa, M. Ishida, T. Nakajima, Y. Honda, O. Kitao, H. Nakai, T. Vreven, J. A. Montgomery, Jr., J. E. Peralta, F. Ogliaro, M. Bearpark, J. J. Heyd, E. Brothers, K. N. Kudin, V. N. Staroverov, T. Keith, R. Kobayashi, J. Normand, K. Raghavachari, A. Rendell, J. C. Burant, S. S. Iyengar, J. Tomasi, M. Cossi, N. Rega, J. M. Millam, M. Klene, J. E. Knox, J. B. Cross, V. Bakken, C. Adamo, J. Jaramillo, R. Gomperts, R. E. Stratmann, O. Yazyev, A. J. Austin, R. Cammi, C. Pomelli, J. W. Ochterski, R. L. Martin, K. Morokuma, V. G. Zakrzewski, G. A. Voth, P. Salvador, J. J. Dannenberg, S. Dapprich, A. D. Daniels, O. Farkas, J. B. Foresman, J. V. Ortiz, J. Cioslowski, and D. J. Fox, Gaussian 09, Revision E.01, Wallingford CT, **2013**.
2. M. K. Singh, A. Etcheverry-Berríos, J. Vallejo, S. Sanz, J. Martínez-Lillo, G. S. Nichol, P. J. Lusby and E. K. Brechin, *Dalton Trans.*, 2022, **51**, 8377-8381.
3. a) A. D. Becke, *Phys. Rev. A*, 1988, **38**, 3098-3101; b) A. D. Becke, *J. Chem. Phys.*, **1993,** *98*, 5648; c) C. Lee, W. Yang and R. G. Parr, *Phys. Rev. B: Condens. Matter Mater. Phys.*, **1988**, *37*, 785.
4. a) A. Schäfer, H. Horn and R. Ahlrichs, *J. Chem. Phys.*, 1992, **97**, 2571-2577; b) A. Schäfer, C. Huber and R. Ahlrichs, *J. Chem. Phys.*, 1994, **100**, 5829; c) G. E. Scuseria and H. F. Schäfer, *J. Chem. Phys.*, 1989, **90**, 3700.
5. L. Noodleman, *J. Chem. Phys.*, 1981, **74**, 5737.
6. F. Neese, *Wiley Interdiscip. Rev. Comput. Mol. Sci.* 2012, **2**, 73–78.
7. (a) K. Eichkorn, O. Treutler, H. Öhm, M. Häser and R. Ahlrichs, *Chem. Phys. Lett.,* 1995, **242**, 652–660; (b) K. Eichkorn, F. Weigend, O. Treutler and R. Ahlrichs, *Theor. Chem. Acc.,* 1997, **97**, 119–124.
8. (a) C. Angeli, R. Cimiraglia, S. Evangelisti, T. Leininger and J.-P. Malrieu, *J. Chem. Phys.,* 2001, **114**, 10252; (b) C. Angeli, R. Cimiraglia and J.-P. Malrieu, *J. Chem. Phys.,* 2002, **117**, 9138; (c) C. Angeli, R. Cimiraglia and J.-P. Malrieu, *Chem. Phys. Lett.,* 2001, **350**, 297–305.
9. SHAPE, version 2.0; continuous shape measures calculation; Electronic Structure Group, Universiat de Barcelona: Barcelona, Spain, 2010.